

FAST AND ACCURATE COMPUTATION OF THE LOGARITHMIC CAPACITY OF COMPACT SETS

JÖRG LIESEN*, OLIVIER SÈTE†, AND MOHAMED M.S. NASSER‡

Abstract. We present a numerical method for computing the logarithmic capacity of compact subsets of \mathbb{C} , which are bounded by Jordan curves and have finitely connected complement. The subsets may have several components and need not have any special symmetry. The method relies on the conformal map onto lemniscatic domains and, computationally, on the solution of a boundary integral equation with the Neumann kernel. Our numerical examples indicate that the method is fast and accurate. We apply it to give an estimate of the logarithmic capacity of the Cantor middle third set and generalizations of it.

Key words. logarithmic capacity, transfinite diameter, Chebyshev constant, conformal map, lemniscatic domain, boundary integral equation

AMS subject classifications. 65E05, 30C30, 30C85, 31A15

1. Introduction. The *logarithmic capacity* $c(E)$ of a compact set E in the complex plane \mathbb{C} is an important invariant that is closely related to polynomial approximation, potential theory, and conformal mapping. If E is simply connected, then $c(E)$ can be obtained via the Riemann map from the complement of E onto the complement of the unit disk. The Riemann map is known analytically for some simple sets such as disks, ellipses and intervals. This leads to analytic formulas for the logarithmic capacity in terms of the parameters describing the corresponding sets. Some examples are shown in Table 2.1 below; see also [23, p. 135], [24, p. 557] or [16, pp. 172–173].

The logarithmic capacity can be obtained from the (exterior) Schwarz–Christoffel map when E consists of one or several components with polygonal boundaries and has a connected complement; see, e.g., [8, Sections 4.4 and 5.8]. For simply connected sets E this has been implemented in the Schwarz–Christoffel Toolbox [7], where the logarithmic capacity is one of the outputs of the command `extermmap`. We refer to [9] for some interesting examples of polygonal sets with special symmetry properties with respect to the real line.

Considering more complicated sets, in particular the Cantor middle third set, Ransford and Rostand pointed out that computing the capacity is “notoriously hard” [25, p. 1499]. They derived a method for computing upper and lower bounds for the logarithmic capacity, which can in principle be made arbitrarily close to each other. Methods for a direct computation of the logarithmic capacity have been proposed in [6, 27]; also see the survey given in [24]. Interest in numerically computing the logarithmic capacity goes back at least to [5].

In this paper we show that the logarithmic capacity of a fairly wide class of sets can be computed fast and accurately using conformal mapping techniques. The method we present is based on a conformal map from the complement of E onto a lemniscatic domain, which is originally due to Walsh [33] and which represents a direct generalization of the Riemann map to sets E with several components. We derived a numerical method for computing Walsh’s map in [21]. The logarithmic capacity is obtained, almost as a by-product, in the first step

*Institute of Mathematics, Technische Universität Berlin, Straße des 17. Juni 136, 10623 Berlin, Germany (liesen@math.tu-berlin.de).

†Mathematical Institute, University of Oxford, Oxford, OX2 6GG, United Kingdom (olivier.sete@maths.ox.ac.uk). The second author was supported by the European Research Council under the European Union’s Seventh Framework Programme (FP7/2007-2013)/ERC grant agreement no. 291068. The views expressed in this article are not those of the ERC or the European Commission, and the European Union is not liable for any use that may be made of the information contained here.

‡Department of Mathematics, Statistics and Physics, Qatar University, P.O.Box 2713, Doha, Qatar (mms.nasser@qu.edu.qa).

of that method, and without computing the conformal map itself. Because of the practical importance of the logarithmic capacity and the apparent lack of general purpose software for its computation, we here derive a stand-alone method and its MATLAB implementation.

Our method is applicable to any compact set E whose complement in the extended plane is connected and bounded by finitely many (sufficiently smooth) Jordan curves. In particular, it is required neither that E is connected nor that E has special symmetry properties. Going beyond the theory presented in [21], we place a particular emphasis on the treatment of sets E with corners. Moreover, we use a recently developed iterative method for mapping parallel slit domains onto domains exterior to ellipses (see Appendix A) in order to compute approximations of the logarithmic capacity of the classical Cantor middle third set and generalizations of it. Numerous further numerical examples demonstrate that our method is fast and accurate. In our numerical examples with sets for which the logarithmic capacity is known analytically, our method typically yields a computed approximation with a relative error of order 10^{-14} . These computations in MATLAB take at most a few seconds on a standard laptop.

The paper is organized as follows. In Section 2 we summarize major facts about the logarithmic capacity and its relation to conformal mapping. In Section 3 we describe our method for computing the logarithmic capacity and state its MATLAB implementation. In Section 4 we give numerical examples.

2. Background. The *transfinite diameter* of a compact set $E \subset \mathbb{C}$ is defined as

$$d(E) := \lim_{n \rightarrow \infty} d_n(E)^{\frac{2}{n(n-1)}}, \quad \text{where} \quad d_n(E) := \max_{z_1, \dots, z_n \in E} \prod_{1 \leq k < \ell \leq n} |z_k - z_\ell|. \quad (2.1)$$

The existence of the limit in (2.1) was first shown by Fekete [10], who considered the d_n a sequence of “generalized diameters” of E . Note that $d_2(E) = \max_{z_1, z_2 \in E} |z_1 - z_2|$ is the (usual) diameter of E . In the same article Fekete showed that the transfinite diameter is equal to the *Chebyshev constant*

$$t(E) := \lim_{n \rightarrow \infty} t_n^{\frac{1}{n}}, \quad \text{where} \quad t_n := \min_{\deg(p) \leq n-1} \max_{z \in E} |z^n - p(z)|. \quad (2.2)$$

Thus, the geometric constant $d(E)$ is closely related to polynomial approximation in the complex plane. This relation can be used to easily show that for both the Chebyshev constant and the transfinite diameter it is sufficient to consider compact sets E with a connected complement. Let $E \subset \mathbb{C}$ be a compact set and let $E^c := \widehat{\mathbb{C}} \setminus E$ denote its complement in the extended complex plane $\widehat{\mathbb{C}} = \mathbb{C} \cup \{\infty\}$. Denote by \mathcal{K} the component of the complement that contains the point at infinity (i.e., $\infty \in \mathcal{K}$) and define $\widehat{E} = \widehat{\mathbb{C}} \setminus \mathcal{K}$. Intuitively, \widehat{E} is obtained after “filling in the holes” in E . Now the definition of the Chebyshev constant and the maximum modulus principle imply that $d(E) = t(E) = t(\widehat{E}) = d(\widehat{E})$.

Szegő [32] showed that if the complement of a compact set E is connected and regular in the sense that it possesses a Green’s function g_{E^c} with pole at infinity, then the transfinite diameter and the Chebyshev constant are equal to the *logarithmic capacity*¹

$$c(E) := \lim_{z \rightarrow \infty} \exp(\log|z| - g_{E^c}(z)). \quad (2.3)$$

Saff [28] called the result $d(E) = t(E) = c(E)$ the *fundamental theorem of classical potential theory*.

¹More precisely, Szegő showed that $d(E)$ is equal to the *Robin constant* γ , which he defined via $\lim_{z \rightarrow \infty} (\log|z| - g_{E^c}(z)) = \log \gamma$. In the modern literature the definition of the Robin constant usually gives $c(E) = \exp(-\gamma)$.

| E | $c(E)$ |
|--------------------------------------|--|
| disk of radius r | r |
| half-disk of radius r | $4r/3^{3/2}$ |
| ellipse with semi-axes a and b | $\frac{1}{2}(a + b)$ |
| line segment of length h | $\frac{1}{4}h$ |
| square with side h | $\frac{1}{4}\Gamma(1/4)^2 h/\pi^{3/2}$ |
| two intervals $[-b, -a] \cup [a, b]$ | $\frac{1}{2}\sqrt{b^2 - a^2}$ |

TABLE 2.1

Examples of known logarithmic capacities.

If $E^c = \widehat{\mathbb{C}} \setminus E$ is simply connected (and E is not a single point), then its Green's function is given by $g_{E^c}(z) = \log|\Phi(z)|$, where $w = \Phi(z)$ is the uniquely determined Riemann map from the complement of E to the complement of the unit disk that is normalized by $\Phi(\infty) = \infty$ and $\Phi'(\infty) > 0$. Near infinity this map can be written as

$$\Phi(z) = \frac{z}{\mu} + \mu_0 + O\left(\frac{1}{z}\right),$$

where $1/\Phi'(\infty) = \mu > 0$ is called the *conformal radius* of E . Hence we have

$$d(E) = t(E) = c(E) = \lim_{z \rightarrow \infty} \exp(\log|z| - \log|\Phi(z)|) = \mu,$$

which shows that the logarithmic capacity can be obtained using (analytical or numerical) conformal mapping techniques. The simplest example is a disk E of radius $r > 0$, for which $\Phi(z) = z/r$ and thus $c(E) = r$; see Table 2.1 for some further analytically known examples.

Walsh [33] proved a direct generalization of the classical Riemann mapping theorem in which he replaced the complement of the unit disk by a *lemniscatic domain* of the form

$$\mathcal{L} := \{z \in \widehat{\mathbb{C}} : |U(z)| > \mu\}, \quad \text{where} \quad U(z) := \prod_{j=1}^{\ell} (z - a_j)^{m_j}, \quad (2.4)$$

$a_1, \dots, a_\ell \in \mathbb{C}$ are pairwise distinct, m_1, \dots, m_ℓ are positive real numbers with $\sum_{j=1}^{\ell} m_j = 1$, and $\mu > 0$. A simple calculation shows that $\log|U(z)| - \log(\mu)$ is the Green's function with pole at infinity for \mathcal{L} , so that by (2.3) we have

$$c(\widehat{\mathbb{C}} \setminus \mathcal{L}) = \lim_{z \rightarrow \infty} \exp(\log|z| - \log|U(z)| + \log(\mu)) = \mu.$$

Walsh proved the following existence theorem in [33].

THEOREM 2.1. *Let E be a compact set whose complement $\mathcal{K} = \widehat{\mathbb{C}} \setminus E$ is connected and bounded by ℓ Jordan curves. Then there exists a uniquely determined lemniscatic domain \mathcal{L} of the form (2.4) with $\mu = c(E)$ and a uniquely determined conformal map*

$$\Phi : \mathcal{K} \rightarrow \mathcal{L} \quad \text{with} \quad \Phi(z) = z + O\left(\frac{1}{z}\right) \quad \text{near infinity.}$$

The first analytic examples of Walsh's conformal map onto lemniscatic domains have recently been given in [30]. These were applied in [31] in a study of polynomial approximation problems on disconnected compact sets and, in particular, two real intervals. In [21] we developed a numerical method for computing the lemniscatic domain \mathcal{L} and the conformal map Φ corresponding to a given compact set E with connected complement \mathcal{K} .

3. Computing the logarithmic capacity. As indicated in the formulation of Theorem 2.1, the logarithmic capacity occurs naturally as one of the parameters defining the lemniscatic domain \mathcal{L} onto which $\mathcal{K} = \widehat{\mathbb{C}} \setminus E$ is mapped. Hence the map Φ itself is not required for computing $c(E)$. A closer inspection of the numerical method developed in [21] shows that the parameters m_1, \dots, m_ℓ, μ of \mathcal{L} are indeed computed in a step that can be executed separately. Due to the structure of the underlying equations the computation of these parameters can be done in a very efficient way. We will now briefly describe this computation. A detailed derivation is given in [21].

As in Theorem 2.1, let E be compact with a finitely connected complement \mathcal{K} . (As noted in Section 2, the connectedness of \mathcal{K} is no restriction for computing the capacity.) We assume that the boundary $\Gamma = \partial E = \partial \mathcal{K}$ of E consists of ℓ Jordan curves $\Gamma_1, \dots, \Gamma_\ell$, which satisfy the following smoothness assumption: Each Γ_j is parameterized by a 2π -periodic function $\eta_j : J_j := [0, 2\pi] \rightarrow \Gamma_j$, which is twice continuously differentiable and satisfies $\dot{\eta}_j(t) = \frac{d\eta_j}{dt}(t) \neq 0$ for all t . These assumptions can be relaxed so as to include domains with corners, see the precise statement and discussion below. The boundary of E is oriented clockwise, so that \mathcal{K} is to the left of the boundary.

Then a parameterization for the whole boundary Γ is given by the map

$$\eta : J \rightarrow \Gamma = \bigcup_{j=1}^{\ell} \Gamma_j, \quad \eta(t) = \begin{cases} \eta_1(t), & t \in J_1, \\ \vdots \\ \eta_\ell(t), & t \in J_\ell, \end{cases} \quad (3.1)$$

where J is the disjoint union of the intervals J_1, \dots, J_ℓ , i.e., J consists of ℓ copies of $[0, 2\pi]$.

For each $j = 1, 2, \dots, \ell$, we choose an auxiliary point α_j in the interior of the Jordan curve Γ_j , and define the function

$$\gamma_j(t) = -\log|\eta(t) - \alpha_j|, \quad t \in J. \quad (3.2)$$

In practical applications of our method the parameters α_j must be specified by the user; cf. the MATLAB code shown in Figure 3.1 below. Our numerical experience with the method suggests that the actual values of the α_j are not important, as long as these points are sufficiently far away from the boundary Γ_j . In the experiments discussed in Section 4 we always chose α_j close to (or at) the center of the interior of Γ_j . The (blue) dots in Figures 4.2 and 4.3 show some examples.

Let H denote the space of all functions f in J , whose restriction to $J_j = [0, 2\pi]$ is a real-valued, 2π -periodic and Hölder continuous function for each $j = 1, 2, \dots, \ell$. Define the integral operators

$$\begin{aligned} (\mathbf{N}f)(s) &= \int_J \frac{1}{\pi} \operatorname{Im} \left(\frac{\dot{\eta}(t)}{\eta(t) - \eta(s)} \right) f(t) dt, \quad s \in J, \\ (\mathbf{M}f)(s) &= \int_J \frac{1}{\pi} \operatorname{Re} \left(\frac{\dot{\eta}(t)}{\eta(t) - \eta(s)} \right) f(t) dt, \quad s \in J, \end{aligned}$$

on H . The kernel of \mathbf{N} is called the *Neumann kernel*. Denoting by \mathbf{I} the identity operator on H , we can state the following theorem that combines [21, Theorems 4.1 and 4.3].

THEOREM 3.1. *For each $j = 1, 2, \dots, \ell$ the integral equation*

$$(\mathbf{I} - \mathbf{N})\mu_j = -\mathbf{M}\gamma_j \quad (3.3)$$

with γ_j as in (3.2) has a unique solution $\mu_j \in H$, and the function

$$h_j := (\mathbf{M}\mu_j - (\mathbf{I} - \mathbf{N})\gamma_j)/2 \quad (3.4)$$

is real-valued and piecewise constant, that is

$$h_j(t) = h_{k,j}, \quad t \in J_k, \quad k = 1, 2, \dots, \ell.$$

Furthermore, $\log(\mu)$ and the parameters m_1, \dots, m_ℓ in (2.4) are the unique solution of the linear algebraic system

$$\begin{bmatrix} h_{1,1} & h_{1,2} & \cdots & h_{1,\ell} & -1 \\ h_{2,1} & h_{2,2} & \cdots & h_{2,\ell} & -1 \\ \vdots & \vdots & \ddots & \vdots & \vdots \\ h_{\ell,1} & h_{\ell,2} & \cdots & h_{\ell,\ell} & -1 \\ 1 & 1 & \cdots & 1 & 0 \end{bmatrix} \begin{bmatrix} m_1 \\ m_2 \\ \vdots \\ m_\ell \\ \log(\mu) \end{bmatrix} = \begin{bmatrix} 0 \\ 0 \\ \vdots \\ 0 \\ 1 \end{bmatrix}. \quad (3.5)$$

This suggests the following method for computing the logarithmic capacity μ :

- (1) For each $j = 1, \dots, \ell$ solve the integral equation (3.3) for the unknown function μ_j .
- (2) Solve the linear algebraic system (3.5) of order $\ell + 1$, where the entries $h_{k,j}$ in the coefficient matrix are computed from (3.4) using the known functions γ_j and the functions μ_j computed in step (1).

The linear algebraic system in step (2) is usually quite small and we solve it directly using the “backslash” operator in MATLAB. Step (1) requires more work:

As described in [21, Section 5], the ℓ boundary integral equations (3.3) can be solved accurately by the Nyström method with the trapezoidal rule. This method yields a linear algebraic system with a dense nonsymmetric matrix $I - B$ of order ℓn , where n is the number of nodes in the discretization of each boundary component. This system can be solved iteratively using the GMRES method. Each step of this method requires one multiplication with the matrix $I - B$. Due to the structure of the integral equation, this product can be computed efficiently in $O(\ell n)$ operations using the Fast Multipole Method (FMM). The eigenvalues of the matrix $I - B$ are contained in the interval $(0, 2]$ and they cluster around 1. As observed in [21] and several other publications (see, e.g., [18, 19]), the number of GMRES iterations for obtaining a very good approximation of the exact solution is mostly independent of the given domain and number of nodes in the discretization of the boundary.

The method for solving (3.3) for the μ_j and subsequently computing h_j in (3.4) has been implemented in the MATLAB function `fbie` shown in [18, Fig. 4.1]. This function uses MATLAB’s built-in `gmres` function as well as the function `zfmmlib2dpart` from the fast multipole toolbox `FMMLIB2D` [11]. The main inputs of the method consist of the discretized functions $\eta(t)$, $\dot{\eta}(t)$, and $\gamma_j(t)$ described above.

For domains with smooth boundaries, we discretize the interval $[0, 2\pi]$ by n nodes s_1, \dots, s_n and write $s = [s_1, \dots, s_n]$ where n is an even integer. For simplicity, we usually take equidistant nodes, i.e.,

$$s_k = (k - 1) \frac{2\pi}{n}, \quad k = 1, \dots, n. \quad (3.6)$$

Then ℓ copies of s give a discretization

$$\mathbf{t} = [s, s, \dots, s]^T \in \mathbb{C}^{\ell n} \quad (3.7)$$

of the parameter domain J , leading to the discretizations

$$\eta(\mathbf{t}) = [\eta_1(s), \eta_2(s), \dots, \eta_\ell(s)]^T, \quad \dot{\eta}(\mathbf{t}), \quad \gamma_j(\mathbf{t}) = -\log|\eta(\mathbf{t}) - \alpha_j| \in \mathbb{C}^{\ell n}, \quad (3.8)$$

$j = 1, 2, \dots, \ell$. We store the discretized functions in the vectors `et`, `etp`, `gam`, respectively, and call

```

function mu = logcapacity(et,etp,alpha)
% Computes the logarithmic capacity of a compact set with L components.
%
% Input:
% et   = [eta_1; ...; eta_L] (discretized boundary; column vector)
% etp  = derivative of the boundary curves (same format as et)
% alpha = [alpha(1); ...; alpha(L)] (auxiliary point alpha(j) interior
%                                     to j-th boundary curve Gamma_j)

L = length(alpha); %% number of boundary components
n = length(et)/L;  %% number of nodes per boundary component

% Auxiliary functions gamma_j(t) = -log |eta(t)-alpha_j|
for k=1:L
    gamj(:,k) = -log(abs(et-alpha(k)));
end

% Compute the auxiliary functions h_j
A = ones(size(et)); %% the function A in the gen. Neumann kernel
for k=1:L
    [~,h_jv(:,k)] = fbie(et,etp,A,gamj(:,k),n,5,[],1e-14,100);
end

% Build and solve linear system for m_1, ..., m_L, log(mu)
for j=1:L
    for k=1:L
        hj(k,j) = sum(h_jv(1+(k-1)*n:k*n,j))/n;
    end
end
matA      = hj;
matA(L+1,1:L) = 1;
matA(1:L,L+1) = -1;
vc_right  = zeros(L+1,1);
vc_right(L+1) = 1;

x = matA\vc_right;
mu = exp(x(L+1));
end

```

FIGURE 3.1. MATLAB code for the computation of the logarithmic capacity.

$[\sim, h] = \text{fbie}(\text{et}, \text{etp}, \text{ones}(\text{size}(\text{et})), \text{gam}, n, 5, [], \text{tol}, \text{maxit})$
Here $[\]$ means that GMRES is used without restart, tol is the convergence criterion used within GMRES, and maxit is the maximal number of GMRES iterations. In the numerical experiments described in Section 4 we have used $\text{tol}=1\text{e}-14$ and $\text{maxit}=100$. The output of fbie are the values $h_j(\mathbf{t})$ of h_j from (3.4), and the values $h_{k,j}$ are computed by taking arithmetic means:

$$h_{k,j} = \frac{1}{n} \sum_{i=1+(k-1)n}^{kn} h_j(t_i), \quad k = 1, 2, \dots, \ell, \quad j = 1, 2, \dots, \ell.$$

These values are used to set up the linear algebraic system (3.5), which we solve directly as mentioned above.

Figure 3.1 shows our MATLAB implementation of the overall method described in this section, where the inputs et and etp are given as in (3.8), and alpha is the column vector of auxiliary points α_j .

The presented method can be extended to domains with corners. We assume that the corner points are not cusps and that the tangent vector of the boundary has only the first kind

discontinuity at these corner points. The left tangent vector at a corner point is considered as the tangent vector at this point. In this case, the solution of the integral equation (3.3) has a singularity in its first derivative in the vicinity of the corner points [22]. Using the equidistant nodes (3.7) to discretize the integrals in (3.3) and (3.4) yields only poor convergence [13, 22, 26]. To achieve a satisfactory accuracy, we discretize the integrals in (3.3) and (3.4) using a *graded mesh* which is based on substituting a new variable in such a way that the discontinuity of the derivatives of the solution of the integral equation at the corner points is removed.

Following Kress [13], we define a bijective, strictly monotonically increasing and infinitely differentiable function, $w : [0, 2\pi] \rightarrow [0, 2\pi]$, by

$$w(t) = 2\pi \frac{v(t)^p}{v(t)^p + v(2\pi - t)^p},$$

where

$$v(t) = \left(\frac{1}{p} - \frac{1}{2}\right) \left(\frac{\pi - t}{\pi}\right)^3 + \frac{1}{p} \frac{t - \pi}{\pi} + \frac{1}{2}.$$

The grading parameter is the integer $p \geq 2$, and the cubic polynomial v is chosen to ensure that, for the equidistant mesh s_1, s_2, \dots, s_n , almost $n/2$ of the grid points $w(s_1), w(s_2), \dots, w(s_n)$ are equally distributed throughout $[0, 2\pi]$, and the other half is accumulated towards the two endpoints 0 and 2π .

Assume that the boundary Γ_k has $q_k > 0$ corner points

$$\eta_k(0), \quad \eta_k(2\pi/q_k), \quad \eta_k(4\pi/q_k), \quad \dots, \quad \eta_k(2(q_k - 1)\pi/q_k).$$

Then we define a bijective, strictly monotonically increasing and infinitely differentiable function, $\delta_k : J_k \rightarrow J_k$, by

$$\delta_k(t) = \begin{cases} w(q_k t)/q_k, & t \in [0, 2\pi/q_k), \\ (w(q_k t - 2\pi) + 2\pi)/q_k, & t \in [2\pi/q_k, 4\pi/q_k), \\ (w(q_k t - 4\pi) + 4\pi)/q_k, & t \in [4\pi/q_k, 6\pi/q_k), \\ \vdots & \\ (w(q_k t - 2(q_k - 1)\pi) + 2(q_k - 1)\pi)/q_k, & t \in [2(q_k - 1)\pi/q_k, 2\pi]. \end{cases}$$

Since the function w has a zero of order p at the endpoints $t = 0$ and $t = 2\pi$ [13, Theorem 2.1], the function δ_k is at least p times continuously differentiable. If the boundary Γ_k has no corner points we define the function $\delta_k(t)$ by

$$\delta_k(t) = t, \quad t \in J_k.$$

Finally, we define a function $\delta : J \rightarrow J$ by

$$\delta(t) = \begin{cases} \delta_1(t), & t \in J_1, \\ \vdots & \\ \delta_\ell(t), & t \in J_\ell. \end{cases}$$

As noted in the first paragraph in [14, p. 242], using the graded mesh

$$\delta(\mathbf{t}) = [\delta_1(s), \delta_2(s), \dots, \delta_\ell(s)]^T \in \mathbb{C}^{\ell n} \quad (3.9)$$

for discretizing the integrals in (3.3) and (3.4) is equivalent to parameterizing the boundary Γ by $\eta(\delta(t))$, and then solving the integral equation as in the case of smooth domains. Hence, we have the discretizations

$$\eta(\delta(\mathbf{t})), \quad \dot{\eta}(\delta(\mathbf{t}))\dot{\delta}(\mathbf{t}), \quad \gamma_j(\delta(\mathbf{t})) = -\log|\eta(\delta(\mathbf{t})) - \alpha_j| \in \mathbb{C}^{\ell n}, \quad (3.10)$$

$j = 1, 2, \dots, \ell$, which replace the discretized functions in (3.8). In our numerical experiments we have used the grading parameter $p = 3$.

4. Numerical examples. We now present numerical examples that illustrate our method. If not stated otherwise, we use an equidistant discretization of $[0, 2\pi]$. Computations were performed in MATLAB R2013a on an ASUS Laptop with Intel Core i7-4720HQ CPU @ 2.60Ghz 2.59 Ghz and 16 GB RAM using the code shown in Figure 3.1. Computation times were measured with the MATLAB `tic toc` command.

4.1. Sets with one component. EXAMPLE 4.1 (Disk). Let $E_r := \{z \in \mathbb{C} : |z| \leq r\}$ denote the closed disk with radius r and $c(E_r) = r$; see Table 2.1. We use the parametrization

$$\eta : [0, 2\pi] \rightarrow \partial E_r, \quad t \mapsto re^{-it},$$

and $n = 2^8 = 256$ points in the discretization. For $r = 1$ our method computes the exact value $c(E_1) = 1.0$. For $r = 2$ it computes the value 2.000000000000003 , accurate to 14 digits. (The relative error is $1.33 \cdot 10^{-15}$.) Each computation took less than 0.1 s.

EXAMPLE 4.2 (Ellipse). We consider the family of ellipses E_d with semi-axes $a = 1$ and $b = 10^{-d}$, and $c(E_d) = (1 + 10^{-d})/2$; see Table 2.1. A parametrization of the boundary is

$$\eta_d(t) = \cos(t) - i10^{-d} \sin(t), \quad t \in [0, 2\pi].$$

We use $d = 1, 2, 3, 4$ and $n = 2^k$ with $k = 8, 9, \dots, 18$. For $d = 1$ we have $c(E_1) = 0.55$, and the value computed by our method has a relative error smaller than 10^{-13} for every n . For $d = 2, 3, 4$ the relative errors of the computed values are shown in Figure 4.1 (left). We observe that our method is less accurate for larger d , i.e., for “thinner” ellipses. For large d the method still yields a very accurate approximation of $c(E_d)$, but this requires a large increase of the number of discretization points. This may be related to the fact that the auxiliary point inside a “thinner” ellipse is necessarily closer to the boundary of the ellipse (cf. our comments after equation (3.2)). On the right of Figure 4.1 we show the computation times.

EXAMPLE 4.3 (Half-disk). Let $E := \{z \in \mathbb{C} : |z| \leq 1, \text{Im}(z) \geq 0\}$ be the upper half of the unit disk with $c(E) = 4/3^{3/2}$; see Table 2.1. Since the boundary of E has corners, we use a graded mesh as described in Section 3. The following table shows the computed values (correct digits are underlined), relative errors, and computation times for increasing n :

| n | computed capacity | relative error | time (s) |
|----------|--------------------------|-----------------------|----------|
| 2^{10} | <u>0.769800347826294</u> | $1.44 \cdot 10^{-8}$ | 0.1 |
| 2^{11} | <u>0.769800357536609</u> | $1.80 \cdot 10^{-9}$ | 0.2 |
| 2^{12} | <u>0.769800358746887</u> | $2.24 \cdot 10^{-10}$ | 0.4 |
| 2^{13} | <u>0.769800358897939</u> | $2.80 \cdot 10^{-11}$ | 0.5 |
| 2^{14} | <u>0.769800358916802</u> | $3.51 \cdot 10^{-12}$ | 0.8 |
| 2^{15} | <u>0.769800358919097</u> | $5.25 \cdot 10^{-13}$ | 1.5 |
| 2^{16} | <u>0.769800358919667</u> | $2.15 \cdot 10^{-13}$ | 3.7 |
| 2^{17} | <u>0.769800358919514</u> | $1.63 \cdot 10^{-14}$ | 6.1 |

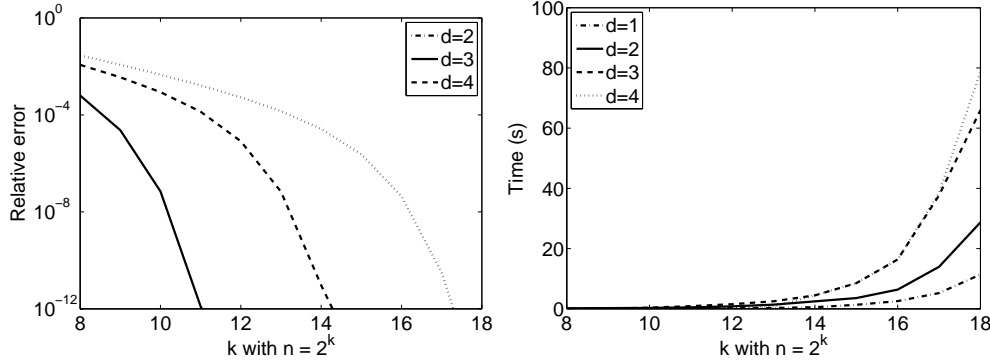


FIGURE 4.1. Results for Example 4.2 (Ellipse): Relative errors of the computed logarithmic capacity (left) and computation times (in seconds, right).

EXAMPLE 4.4 (Square). Let E be the square with vertices $1 + i, 1 - i, -1 - i, -1 + i$ and hence side length $h = 2$, giving $c(E) = \frac{1}{2}\Gamma(1/4)^2/\pi^{3/2}$; see Table 2.1. Evaluating this expression in MATLAB gives $c(E) = 1.180340599016096$, which we use as the “exact” value for our experiment. As for the half-disk, our discretization uses a graded mesh. The following table shows the computed values (correct digits are underlined), relative errors and computation times for increasing n :

| n | computed capacity | relative error | time (s) |
|----------|--------------------------|-----------------------|----------|
| 2^8 | <u>1.180328330582103</u> | $1.04 \cdot 10^{-05}$ | 0.1 |
| 2^9 | <u>1.180339089365394</u> | $1.28 \cdot 10^{-06}$ | 0.1 |
| 2^{10} | <u>1.180340411967884</u> | $1.58 \cdot 10^{-07}$ | 0.1 |
| 2^{11} | <u>1.180340575744745</u> | $1.97 \cdot 10^{-08}$ | 0.2 |
| 2^{12} | <u>1.180340596114299</u> | $2.46 \cdot 10^{-09}$ | 0.2 |
| 2^{13} | <u>1.180340598653831</u> | $3.07 \cdot 10^{-10}$ | 0.5 |
| 2^{14} | <u>1.180340598970863</u> | $3.83 \cdot 10^{-11}$ | 0.6 |
| 2^{15} | <u>1.180340599010508</u> | $4.73 \cdot 10^{-12}$ | 1.1 |
| 2^{16} | <u>1.180340599015215</u> | $7.47 \cdot 10^{-13}$ | 2.3 |
| 2^{17} | <u>1.180340599016100</u> | $3.57 \cdot 10^{-15}$ | 5.9 |

We also compute the logarithmic capacity with the Schwarz–Christoffel Toolbox [7]. With the default settings the commands

```
p = polygon([1+i, -1+i, -1-i, 1-i]);
f = extermat(p);
capacity(f)
```

yield the value 1.180340599090706, which has the relative error $6.32 \cdot 10^{-11}$. For a tolerance of 10^{-14} instead of the default value 10^{-8} the Schwarz–Christoffel Toolbox returns a very accurate result with the relative error $3.76 \cdot 10^{-16}$.

In both Example 4.3 and 4.4 the relative error in our method converges to the machine precision for increasing n . The reason that we need many points to obtain very accurate results is that in both examples the boundaries have corners.

EXAMPLE 4.5. We consider the set in Figure 4.2 (left), which is of the form introduced in [12]. For these sets an analytic parameterization of the boundary and the logarithmic capacity are known explicitly. Here we consider the compact set E bounded by

$$\eta(t) = \psi(e^{-it}), \quad t \in [0, 2\pi],$$

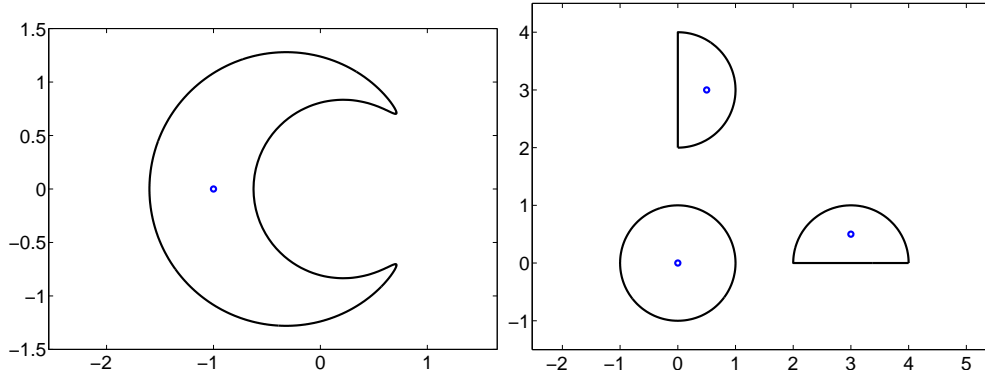


FIGURE 4.2. The sets from Examples 4.5 (left) and 4.8 (right). The (blue) dots show the auxiliary points α_j .

where ψ is the conformal map given by [12, Equation (3.2)] with the parameters $\lambda_m = 1$, $\phi = \pi/2$ and $\epsilon = 0.1$. Then $c(E) = 1.223502096192244$; see [12, Corollary 3.4]. The following table shows the computed values (correct digits are underlined), relative errors and computation times for increasing n :

| n | computed capacity | relative error | time (s) |
|----------|--------------------------|-----------------------|----------|
| 2^8 | <u>1.223385602611070</u> | $9.52 \cdot 10^{-05}$ | 0.1 |
| 2^9 | <u>1.223500703601890</u> | $1.14 \cdot 10^{-06}$ | 0.1 |
| 2^{10} | <u>1.223502095786708</u> | $3.31 \cdot 10^{-10}$ | 0.1 |
| 2^{11} | <u>1.223502096192245</u> | $3.63 \cdot 10^{-16}$ | 0.2 |

As in the two previous examples, the relative error converges to machine precision as n increases. The reason that we need many points to obtain an accurate result is different from the two previous examples. Here the boundary is analytic, but with equispaced points in $[0, 2\pi]$ and the above parametrization, only few discretization points lie on the inner arc, which is not well resolved for smaller n . Here, a different parametrization might lead to very accurate results already for small n , but we did not pursue this further.

4.2. Sets with several components. EXAMPLE 4.6 (Two disks with equal radii). Let $r, z_0 \in \mathbb{R}$ with $0 < r < z_0$ and let E be the union of the two disks $D_r(z_0) = \{z \in \mathbb{C} : |z - z_0| \leq r\}$ and $D_r(-z_0) = \{z \in \mathbb{C} : |z + z_0| \leq r\}$. From [30, Theorem 4.2] we know that

$$c(E) = \frac{2K}{\pi} \sqrt{z_0^2 - r^2} \sqrt{2L(1 + L^2)},$$

where

$$\rho = \frac{\sqrt{z_0 + r} - \sqrt{z_0 - r}}{\sqrt{z_0 + r} + \sqrt{z_0 - r}}, \quad L = 2\rho \prod_{k=1}^{\infty} \left(\frac{1 + \rho^{8k}}{1 + \rho^{8k-4}} \right)^2,$$

and

$$K = K(L^2) = \int_0^1 \frac{1}{\sqrt{(1-t^2)(1-L^4t^2)}} dt.$$

The product for L converges very quickly, so that it suffices to compute the first few factors to obtain the correct value up to the machine precision. Using this value of L we evaluate the

complete elliptic integral of the first kind for K with the MATLAB command `ellipk`. We use the result as the “exact” value $c(E)$. The constant L can also be written with the Jacobi theta functions as $L = \theta_2(0; \rho^4)/\theta_3(0; \rho^4)$, using their product representation [34, §21.3]. We apply our algorithm for $z_0 = 1$ and $r = 0.5, 0.7, 0.9$ with $n = 2^8$ (giving $2n = 2^9$ nodes in total). The results are very accurate (14 digits of accuracy) and are shown in the following table (correct digits are underlined):

| r | computed capacity | exact capacity | relative error | time (s) |
|-----|--------------------------|-------------------|-----------------------|----------|
| 0.5 | <u>1.030651235187015</u> | 1.030651235187014 | $8.62 \cdot 10^{-16}$ | 0.1 |
| 0.7 | <u>1.252472555601970</u> | 1.252472555601971 | $1.42 \cdot 10^{-15}$ | 0.1 |
| 0.9 | <u>1.465698640729795</u> | 1.465698640729791 | $2.42 \cdot 10^{-15}$ | 0.1 |

EXAMPLE 4.7 (Two disks with different radii). Let $0 < u < v$ and

$$a = \frac{\sinh(v)}{\sinh(v-u)} \quad \text{and} \quad r = \frac{\sinh(u)}{\sinh(v-u)}.$$

Then the capacity of $E_{a,r} = D_1(0) \cup D_r(a)$, which is the union of two disjoint disks, is

$$c(E_{a,r}) = e^{u^2/v} \sinh(u) \left| \frac{\theta_2(0; e^{-v})\theta_3(0; e^{-v})\theta_4(0; e^{-v})}{\theta_1(iu; e^{-v})} \right|,$$

where $\theta_1, \theta_2, \theta_3, \theta_4$ are the Jacobi theta functions (see below). This formula was brought to our attention by Thomas Ransford, who derived it from the Green’s function of an annulus in [4, Ch. V]. We are not aware of a publication of this result in the literature. The Jacobi theta functions are [34, §21.1]

$$\begin{aligned} \theta_1(z; q) &= 2q^{1/4} \sum_{n=0}^{\infty} (-1)^n q^{n(n+1)} \sin((2n+1)z), \\ \theta_2(z; q) &= 2q^{1/4} \sum_{n=0}^{\infty} q^{n(n+1)} \cos((2n+1)z), \\ \theta_3(z; q) &= 1 + 2 \sum_{n=1}^{\infty} q^{n^2} \cos(2nz), \\ \theta_4(z; q) &= 1 + 2 \sum_{n=1}^{\infty} (-1)^n q^{n^2} \cos(2nz), \end{aligned}$$

and we evaluate them by truncating the series when the absolute value of the terms become smaller than MATLAB’s `eps`. We use the computed value of $c(E_{a,r})$ as the exact capacity. We apply our numerical methods with $n = 2^8$ nodes per boundary, and obtain the very accurate results shown in the following table (correct digits are underlined):

| (u, v) | computed capacity | exact capacity | relative error | time (s) |
|------------|--------------------------|-------------------|-----------------------|----------|
| (0.5, 0.7) | <u>2.991271539541696</u> | 2.991271539541695 | $2.96 \cdot 10^{-16}$ | 0.2 |
| (0.5, 1.0) | <u>1.637069166040759</u> | 1.637069166040759 | $2.72 \cdot 10^{-16}$ | 0.1 |
| (0.5, 1.5) | <u>1.260209159232260</u> | 1.260209159232259 | $1.76 \cdot 10^{-16}$ | 0.1 |

EXAMPLE 4.8. Let E be the union of a disk and two half-disks, as shown in Figure 4.2 (right). We are not aware of an analytic formula for $c(E)$, but it has been shown in [25] that

$$c(E) \in [2.1969933, 2.2003506],$$

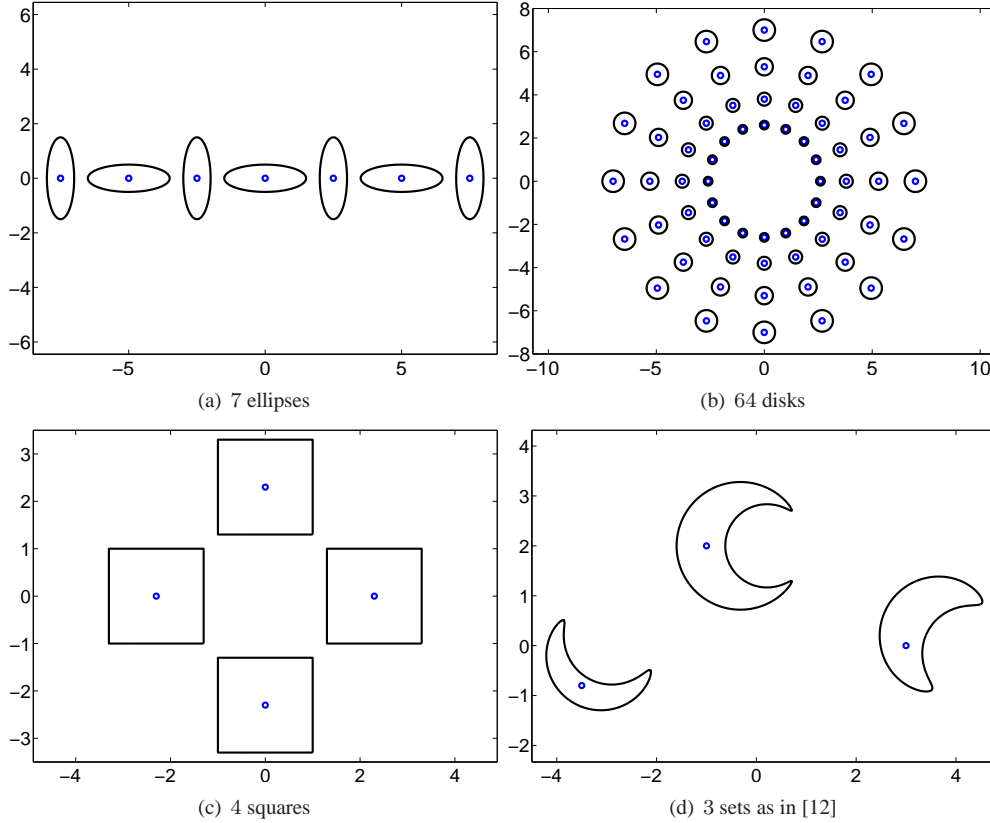


FIGURE 4.3. The sets in Example 4.9. The (blue) dots show the auxiliary points α_j .

and the authors “best guess” is $c(E) \approx 2.19699371717$. We parameterize the circle by $\eta_1(t) = e^{-it}$, and the two half-disks analogously to Example 4.3. With $n = 2^{10}$ nodes per boundary component our method gives the computed value $c(E) \approx 2.196993710282112$ in about 0.9 s. For $n = 2^{16}$ our method computes the value $c(E) \approx 2.196993717171386$ in 36.2 s, and this value matches exactly the estimate from [25].

EXAMPLE 4.9. We consider the compact sets shown in Figure 4.3. These sets were also used in [21, Examples 2–5]. To our knowledge, the logarithmic capacities of these sets are not known analytically. The following table shows the values computed by our method and the computation times:

| E | n | computed capacity | time (s) |
|-------------------|----------|-------------------|----------|
| 7 ellipses | 2^8 | 4.961809958325545 | 1.2 |
| 64 disks | 2^8 | 7.177814562549484 | 43.6 |
| 4 squares | 2^{10} | 3.083190170261768 | 1.3 |
| 3 sets as in [12] | 2^{10} | 2.977866214534663 | 1.1 |

EXAMPLE 4.10 (“The World Islands”). We consider the unbounded domain \mathcal{K} of connectivity $\ell = 210$ exterior to an artificial archipelago located in the waters of the Arabian Gulf, four kilometres off the coast of Dubai, and known as “The World Islands”; see also [18]. An aerial image from *Google Maps* of “The World Islands” is shown in Figure 4.4 (left). The boundaries of the islands extracted from the aerial image are shown in Figure 4.4 (right),

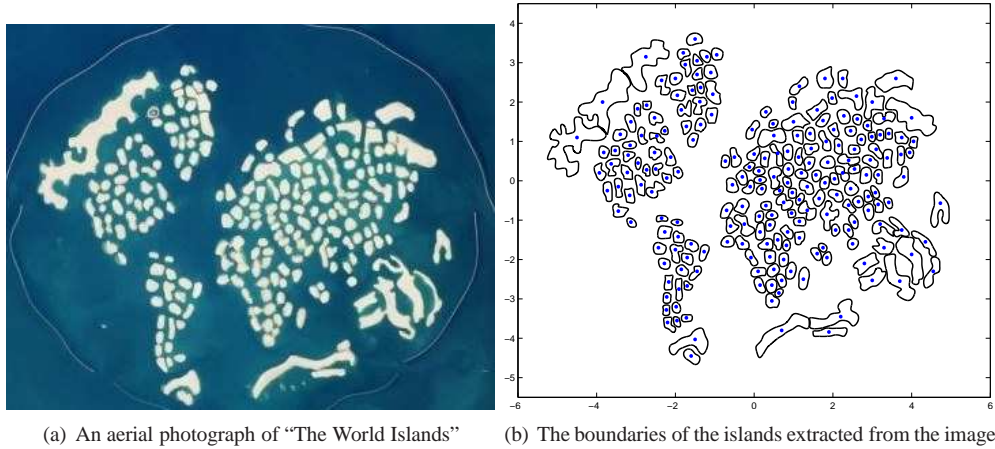


FIGURE 4.4. “The World Islands” from Example 4.10. The (blue) dots show the auxiliary points α_j .

and we parameterize them using trigonometric interpolating polynomials. The boundaries are very close to each other but they do not touch. The following table shows the values computed by our method and the computation times:

| n | computed capacity | time (s) |
|----------|-------------------|----------|
| 2^5 | 4.384226180107323 | 484 |
| 2^6 | 4.388057916386704 | 872 |
| 2^7 | 4.387882300144899 | 1464 |
| 2^8 | 4.387881092385658 | 2813 |
| 2^9 | 4.387881092740317 | 4986 |
| 2^{10} | 4.387881092740335 | 9656 |
| 2^{11} | 4.387881092740328 | 17717 |

4.3. Several real intervals and Cantor sets. In this section we consider sets consisting of several real intervals, and in particular the classical Cantor middle third set and generalizations of it. Our method is not directly applicable to such sets, since these are not bounded by Jordan curves. We overcome this difficulty by considering a preliminary conformal map to “open up” the intervals and obtain a compact set of same logarithmic capacity, but bounded by smooth Jordan curves.

Let E be a set that consists of ℓ real intervals, so that its complement $\mathcal{K} = E^c = \widehat{\mathbb{C}} \setminus E$ is an unbounded domain (containing ∞) bounded by ℓ parallel straight slits, all on the real axis. In order to apply our method, we will first use conformal mappings to compute an unbounded multiply connected domain G exterior to a disjoint union of ℓ ellipses, such that the domains G and \mathcal{K} are conformally equivalent. The computation of G and the conformal map $z = \omega(\zeta)$ from G onto \mathcal{K} is based on a technique developed recently in [20], which we describe in Appendix A. The conformal map is normalized by $\omega(\zeta) = \zeta + O(1/\zeta)$ as $\zeta \rightarrow \infty$, which makes it unique, and also implies $c(E) = c(G^c)$ by [23, Theorem 5.2.3], that is, the capacity of E can be computed as the capacity of the union of the ℓ ellipses. In summary, we use the method described in Appendix A for computing G , and then apply our usual method (as stated in Fig. 3.1) in order to compute an approximation of $c(E) = c(G^c)$.

We start with the much studied case of two real intervals, for which the logarithmic capacity is known analytically. The numerical results for these sets also give an indication of

the accuracy of our method for the Cantor sets, where no analytic formula for their logarithmic capacity is known.

EXAMPLE 4.11 (Two real intervals). Let $E_{a,b} = [-1, a] \cup [b, 1]$ with $-1 < a < b < 1$. When the two intervals have the same length, i.e., when $0 < -a = b < 1$, the exact capacity of $E_{a,b}$ is given by (see Table 2.1)

$$c(E_{a,b}) = \frac{1}{2} \sqrt{1 - a^2}.$$

For the general case, an analytic formula derived by Achieser [1] (see also [29]) has the form

$$c(E_{a,b}) = \frac{1+b}{2(1+a)} \frac{\theta_4(0; q)}{\theta_4(\lambda\pi/2; q)},$$

where

$$k = \sqrt{\frac{2(b-a)}{(1-a)(1+b)}}, \quad k' = \sqrt{1-k^2}, \quad K = K(k), \quad K' = K(k'), \quad q = e^{-\pi K'/K},$$

$K(k)$ is the complete elliptic integral of the first kind (see Example 4.6 above), θ_4 is the fourth Jacobi theta function (see Example 4.7 above), and $0 < \lambda < K$ is defined uniquely by the Jacobi elliptic function sn as

$$\text{sn}(\lambda, k) = \sqrt{\frac{1-a}{2}}.$$

We compute the values of $K(k)$, $K(k')$, and θ_4 as explained in Examples 4.6 and 4.7. The value of the parameter λ is computed using the MATLAB function `asne`, i.e.,

$$\lambda = \text{asne}(\sqrt{(1-a)/2}, k).$$

As explained above, we use our method to compute $c(G^c) = c(E_{a,b})$, where G is a domain bounded by smooth Jordan curves that is found by “opening up” the real intervals. Very accurate results are obtained with only $n = 2^8$ nodes per boundary, as shown in the following table (correct digits are underlined):

| (a, b) | computed capacity | exact capacity | relative error | time (s) |
|-----------------|--------------------------|-------------------|-----------------------|----------|
| $(-0.5, -0.1)$ | <u>0.488829271154718</u> | 0.488829271154715 | $4.77 \cdot 10^{-15}$ | 2.9 |
| $(0.5, 0.6)$ | <u>0.499101557166360</u> | 0.499101557166361 | $1.11 \cdot 10^{-15}$ | 3.5 |
| $(-0.5, 0.3)$ | <u>0.457718411572721</u> | 0.457718411572721 | $8.49 \cdot 10^{-16}$ | 2.7 |
| $(-0.5, 0.5)$ | <u>0.433012701892217</u> | 0.433012701892219 | $5.64 \cdot 10^{-15}$ | 2.1 |
| $(-0.01, 0.01)$ | <u>0.499974999374968</u> | 0.499974999374969 | $8.88 \cdot 10^{-16}$ | 3.6 |

As a final remark concerning this example, it is worth mentioning that an analytic formula for the logarithmic capacity of sets consisting of several intervals has been derived recently in [3].

EXAMPLE 4.12 (Cantor middle third set). In this example we consider the classical Cantor middle third set. Let $E_0 = [0, 1]$ and recursively define

$$E_k := \frac{1}{3}E_{k-1} \cup \left(\frac{1}{3}E_{k-1} + \frac{2}{3} \right), \quad k \geq 1.$$

This means that E_k is constructed by “removing” the middle one third of each interval that E_{k-1} consists of. Then the Cantor middle third set is defined as $E := \bigcap_{k=1}^{\infty} E_k$. While no

analytic formula for $c(E)$ is known, several attempts have been made to numerically approximate $c(E)$. In [25] it is shown that

$$c(E) \in [0.22094810685, 0.22095089228],$$

and based on several of their computed values, Ransford and Rostand wrote that their “best guess” is

$$c(E) \approx 0.220949102189507.$$

Using two different approaches based on Schwarz-Christoffel mappings, Banjai, Embree, and Trefethen computed $c(E_k)$ for $k = 1, 2, \dots, 9$, and extrapolating from their computed values they obtained $c(E) \approx 0.2209491^2$. Recently, Krüger and Simon [15] obtained the value $c(E) \approx 0.22094998647421$ in a study of the spectral theory of orthogonal polynomials associated to the Cantor measure. Referring to their result they noted that one “should only trust the first six digits or so”.

We will now describe our approach for computing an approximation of $c(E)$. Similar to Banjai, Embree and Trefethen, we will compute $c(E_k)$ for a few small values of k , and then obtain an approximation of $c(E)$ by extrapolation. We compute the capacities $c(E_k)$ with the open-up method described in the beginning of Section 4.3. The resulting values and computation times for $k = 1, 2, \dots, 12$ are shown in the following table:

| k | $\ell = 2^k$ | computed capacity | time (s) |
|-----|--------------|-------------------|----------|
| 1 | 2 | 0.235702260395518 | 1.0 |
| 2 | 4 | 0.228430704425426 | 1.5 |
| 3 | 8 | 0.224752818755436 | 2.5 |
| 4 | 16 | 0.222887290751916 | 4.1 |
| 5 | 32 | 0.221938129124324 | 7.3 |
| 6 | 64 | 0.221454205006181 | 15.7 |
| 7 | 128 | 0.221207178734289 | 44.6 |
| 8 | 256 | 0.221080995391656 | 148.0 |
| 9 | 512 | 0.221016516406108 | 565.1 |
| 10 | 1024 | 0.220983561713855 | 2375.9 |
| 11 | 2048 | 0.220966717159289 | 9128.4 |
| 12 | 4096 | 0.220958106742622 | 34984.7 |

In order to extrapolate from our computed values, we note that the differences

$$d_k = c(E_k) - c(E_{k+1}), \quad k = 1, 2, \dots, 11$$

behave linearly on a logarithmic scale; see the (blue) circles in Figure 4.5. We therefore use the MATLAB command `p=polyfit(1:11, log(d(1:11)), 1)` for computing a linear interpolant $p(x) = p_1x + p_2$ of the values $\log(d_k)$. The computed coefficients are

$$p_1 = -0.673356333942526, \quad p_2 = -4.26116079806122,$$

and the values $p(k)$ for all $k = 1, 2, \dots, 48$, where $p(48) \approx 10^{-16}$, are shown by the (black) pluses in Figure 4.5. Since $p(k) \approx \log(d_k)$, we can find an approximation of $c(E_k)$ for each $k = 13, 14, \dots$ by extrapolation starting with our computed value for $c(E_{12})$, and obtain

$$c(E_k) = c(E_{12}) - \sum_{j=12}^{k-1} \exp(p(j)), \quad k \geq 13.$$

²These computations, made in July 2005, were also reported in [25].

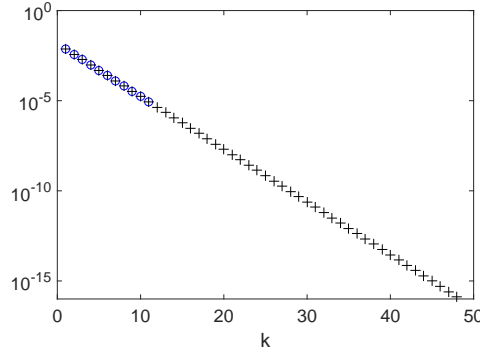


FIGURE 4.5. The values $d_k = c(E_k) - c(E_{k+1})$ for $k = 1, 2, \dots, 11$ (circles) and the values $\exp(p(k))$ for $k = 1, 2, \dots, 48$ (pluses); see Example 4.12.

Since $p(49) < 10^{-16}$, we use only the values up to $p(48)$, which gives our estimate for the capacity of the Cantor middle third set as

$$c(E) \approx 0.220949194629475.$$

This estimate agrees up to the seventh digit with the estimates of Ransford and Rostand as well as Banjai, Embree and Trefethen.

EXAMPLE 4.13 (Generalized Cantor set). As in [25, Section 6] we will now generalize the construction of the Cantor middle third set as follows. Let $r \in (0, 0.5)$ and $E_0^r := [0, 1]$. Recursively define

$$E_k^r := rE_{k-1}^r \cup (rE_{k-1}^r + (1-r)), \quad k \geq 1,$$

and let $E^r := \bigcap_{k=0}^{\infty} E_k^r$. The parameter r determines how much is removed from each interval of E_{k-1}^r in order to obtain E_k^r . If we want to remove the middle $q \in (0, 1)$, we need to set $r = (1-q)/2$. For $q = 1/3$ we have $r = 1/3$ and hence $E^{1/3}$ is the classical Cantor middle third set. The limiting cases are $E^0 = \{0, 1\}$ with $c(E^0) = 0$, and $E^{1/2} = [0, 1]$ with $c(E^{1/2}) = 1/4$; see Table 2.1.

Using exactly the same approach as described in Example 4.12 we have computed the following approximations of $c(E^r)$:

| q | r | computed capacity |
|------|-------|-------------------|
| 3/4 | 1/8 | 0.109156838696175 |
| 2/3 | 1/6 | 0.13844418298159 |
| 1/2 | 1/4 | 0.186511016338442 |
| 1/3 | 1/3 | 0.220949194629475 |
| 1/4 | 3/8 | 0.233218551525021 |
| 1/5 | 2/5 | 0.23901897053678 |
| 1/6 | 5/12 | 0.242233234580321 |
| 1/7 | 3/7 | 0.244206003640726 |
| 1/8 | 7/16 | 0.245506481568117 |
| 1/9 | 4/9 | 0.246410328817 |
| 1/10 | 9/20 | 0.247064652445187 |
| 1/11 | 10/22 | 0.247553947239903 |
| 1/12 | 11/24 | 0.247929630663845 |

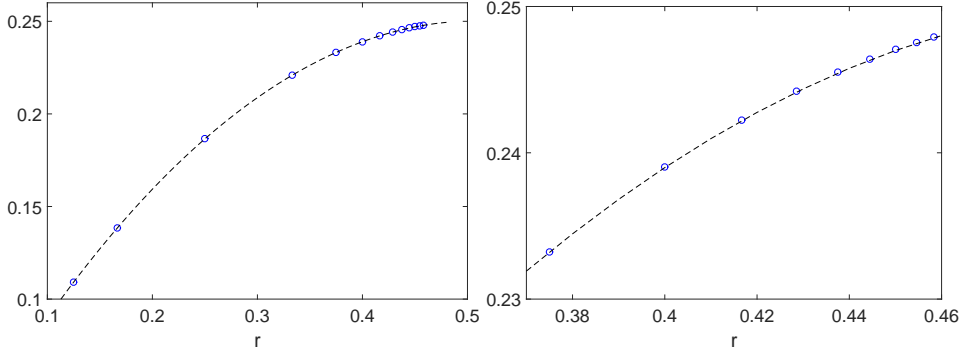


FIGURE 4.6. Computed approximation of $c(E^r)$ (circles) and the function $f(r)$ (dashed); see Example 4.13.

The (blue) circles in Figure 4.6 show our computed approximations of $c(E^r)$, where the right part of the figure is a closeup of the left part. The dashed line shows the function

$$f(r) = r(1-r) - \frac{r^3}{2} \left(\frac{1}{2} - r \right)^{3/2},$$

which was suggested in [25] as an approximation of $c(E^r)$. The maximum distance between the values of $f(r)$ and our computed approximations of $c(E^r)$ is $7.5189 \cdot 10^{-5}$. Thus, similar to computations reported in [25], the function $f(r)$ very closely approximates our computed approximations of $c(E^r)$.

5. Concluding remarks. We have presented a numerical method for the computation of the logarithmic capacity of compact sets bounded by Jordan curves in the complex plane. These sets may consist of several components and need not have any special symmetry properties. In several numerical examples with sets for which the logarithmic capacity is known analytically, our method yields a computed approximation with a relative error close to the machine precision. For “simple” sets, in particular simply connected ones, the computations in MATLAB take at most a few seconds.

Let us point out a few open questions. From a computational point of view, an automated choice of the auxiliary points α_j (interior to each boundary curve) would be of interest. The numerical experiments for compact sets where the logarithmic capacity is known analytically suggest that the method is fast and accurate. A formal analysis of the numerical stability and accuracy of our method is beyond the scope of this article and remains a subject of further work. To compute an approximation of the capacity of the Cantor sets, we devised an ad hoc method to “open up” the intervals by conformal mapping and obtain a domain bounded by Jordan curves, to which our method could be applied. It would be of interest to devise an “open-up method” for general Jordan arcs that is computationally tractable.

Appendix A. Numerical computation of the preimage of a parallel slit domain.

Let Ω be a given parallel slit domain, i.e., the entire z -plane with m slits L_j , $j = 1, 2, \dots, \ell$, along straight lines; see the top of Figure A.1. An efficient numerical method for computing the conformal map $z = \omega(\zeta)$ from an unbounded domain G exterior to ℓ smooth Jordan curves Γ_j , $j = 1, 2, \dots, \ell$, onto the parallel slit domain Ω such that $\omega(\zeta) = \zeta + O(1/\zeta)$ as $\zeta \rightarrow \infty$ has been presented in [17, Section 4.5]. Assume that the boundary Γ of G is parametrized by the function $\eta(t)$ as in (3.1). Assume also the operators \mathbf{N} and \mathbf{M} are the

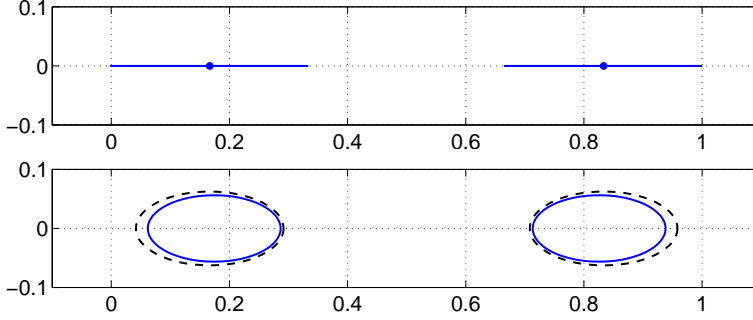


FIGURE A.1. The given parallel slit domain Ω (top), the initial preimage domain G^0 (dashed line, bottom), and the computed preimage domain G (solid line, bottom).

same operators as in (3.3). Then we have the following theorem from [17].

THEOREM A.1. *Let*

$$\gamma(t) = \text{Im}[\eta(t)], \quad t \in J, \quad (\text{A.1})$$

let μ be the unique solution of the boundary integral equation

$$(\mathbf{I} - \mathbf{N})\mu = -\mathbf{M}\gamma, \quad (\text{A.2})$$

and let h be the piecewise constant function

$$h = (\mathbf{M}\mu - (\mathbf{I} - \mathbf{N})\gamma)/2. \quad (\text{A.3})$$

Then the function f with the boundary values

$$f(\eta(t)) = \gamma(t) + h(t) + i\mu(t) \quad (\text{A.4})$$

is analytic in G with $f(\infty) = 0$ and the conformal mapping ω is given by

$$\omega(\zeta) = \zeta - if(\zeta), \quad \zeta \in G \cup \Gamma. \quad (\text{A.5})$$

In Theorem A.1, the domain G is assumed to be known, and the integral equation (A.2) is used to find the conformal map $z = \omega(\zeta)$ from G onto the parallel slit domain $\Omega = \omega(G)$. In our application with the Cantor sets, however, the domain G is unknown and the parallel slit domain Ω is known. Hence a straightforward application of a numerical method based on Theorem A.1 is not possible.

We will now describe an iterative method developed in [20] for computing G and the conformal map from G onto the (known) parallel slit domain Ω . The method is an improvement of a numerical method suggested by Aoyama, Sakajo, and Tanaka [2], where the preimage G is assumed to be circular. Since the image region Ω is elongated (parallel slit domain), crowding can cause serious problems. Further, the convergence of the iterative method is slow if G is assumed to be circular. To overcome such difficulties, it was assumed in [20] that the boundaries of the domain G are ellipses instead of circles.

Let $|L_j|$ denote the length of the slit L_j and let z_j denote its center, $j = 1, 2, \dots, \ell$. In the iteration step $i = 0, 1, 2, \dots$ we assume that the domain G^i is a multiply connected domain bounded by the ellipses Γ_j^i , parametrized for $j = 1, 2, \dots, \ell$ by

$$\eta_j^i(t) = \zeta_j^i + 0.5(a_j^i \cos t - ib_j^i \sin t), \quad t \in J_j = [0, 2\pi].$$

Then the following iteration computes the centers of the ellipses ζ_j^i , the lengths of the major axes a_j^i , and the lengths of the minor axes b_j^i for $j = 1, 2, \dots, \ell$.

Initialization:

Let $\varepsilon > 0$ be a given tolerance and let Max be a maximum number of iterations. (In our numerical experiments in this paper we always used $\varepsilon = 10^{-14}$ and $Max = 50$.) Set

$$\zeta_j^0 = z_j, \quad a_j^0 = (1 - 0.5r)|L_j|, \quad b_j^0 = ra_j^0,$$

where $0 < r < 1$ is the ratio of the lengths of the major and minor axes of the ellipse (see Figure A.1 (dashed line, bottom) for $r = 0.5$).

For $i = 1, 2, \dots$:

1. Map G^{i-1} to a parallel slit domain Ω^i (based on Theorem A.1), which is the entire z -plane with ℓ slits L_j^i , $j = 1, 2, \dots, \ell$, along horizontal straight lines.
2. If $|L_j^i|$ denotes the length of the slit L_j^i and z_j^i denotes its center, then we define the parameters of the preimage domain G^i as

$$\zeta_j^i = \zeta_j^{i-1} - (z_j^i - z_j), \tag{A.6}$$

$$a_j^i = a_j^{i-1} - (|L_j^i| - |L_j|), \tag{A.7}$$

$$b_j^i = ra_j^i. \tag{A.8}$$

3. Stop the iteration if

$$\max_{1 \leq j \leq m} (|z_j^i - z_j| + ||L_j^i| - |L_j||) < \varepsilon \quad \text{or} \quad i > Max$$

Several numerical examples in this paper as well as in [2, 20] show the convergence of this iterative method, but no proof of convergence has been given so far. Numerical experiments also show that the iterative method requires fewer iterations for small values of r , which means that the ellipses will be thin. For thin ellipses, however, we usually need a larger number of points n for discretizing the boundary integral equations and the GMRES method for solving these discretized equations requires more iterations to converge.

In the numerical experiments with the Cantor sets shown in this paper we have not chosen to optimize upon these parameters, but we used the fixed values $r = 0.5$ and $n = 64$. The number of iterations for the convergence to the accuracy $\varepsilon = 10^{-14}$ of the above iterative method applied in the computation of $c(E_k)$ for $k = 1, 2, \dots, 12$ is shown in Figure A.2. The (unpreconditioned) GMRES method for solving the discretized integral equations required between 5 and 11 iterations.

Acknowledgments. We thank Nick Trefethen for sharing the numerical results on the capacity of the Cantor middle third set he obtained together with Banjai and Embree. We thank Thomas Ransford for bringing to our attention the analytic formula for the capacity of two unequal disks (Example 4.7).

REFERENCES

- [1] N. ACHIESER, *Sur les polynomes de Tchebycheff pour deux segments.*, C. R. Acad. Sci., Paris, 191 (1930), pp. 754–756.
- [2] N. AOYAMA, T. SAKAJO, AND H. TANAKA, *A computational theory for spiral point vortices in multiply connected domains with slit boundaries*, Jpn. J. Ind. Appl. Math., 30 (2013), pp. 485–509.
- [3] A. B. BOGATYREV AND O. A. GRIGORIEV, *Capacity of several aligned segments*, ArXiv: 1512.07154, (2015).
- [4] R. COURANT AND D. HILBERT, *Methods of mathematical physics. Vol. I*, Interscience Publishers, Inc., New York, N.Y., 1953.

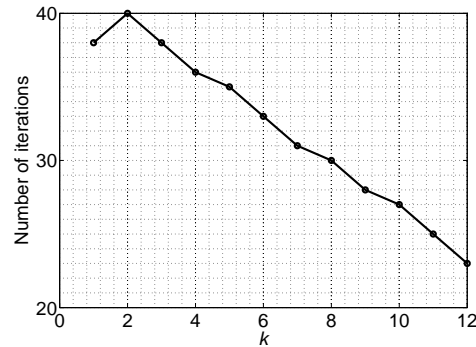


FIGURE A.2. Number of iterations for computing the preimage domains required in the computation of $c(E_k)$ for $k = 1, 2, \dots, 12$.

- [5] P. DAVIS, *Numerical computation of the transfinite diameter of two collinear line segments.*, J. Res. Natl. Bur. Stand., 58 (1957), pp. 155–156.
- [6] W. DIJKSTRA AND M. HOCHSTENBACH, *Numerical approximation of the logarithmic capacity*, CASA report, (2009), pp. 08–09.
- [7] T. A. DRISCOLL, *Schwarz–Christoffel Toolbox User’s Guide. Version 2.3*, available from <http://www.math.udel.edu/~driscoll/SC/guide.pdf>.
- [8] T. A. DRISCOLL AND L. N. TREFETHEN, *Schwarz–Christoffel mapping*, vol. 8 of Cambridge Monographs on Applied and Computational Mathematics, Cambridge University Press, Cambridge, 2002.
- [9] M. EMBREE AND L. N. TREFETHEN, *Green’s functions for multiply connected domains via conformal mapping*, SIAM Rev., 41 (1999), pp. 745–761.
- [10] M. FEKETE, *Über die Verteilung der Wurzeln bei gewissen algebraischen Gleichungen mit ganzzahligen Koeffizienten*, Math. Z., 17 (1923), pp. 228–249.
- [11] L. GREENGARD AND Z. GIMBUTAS, *FMMLIB2D: A MATLAB toolbox for fast multipole method in two dimensions, Version 1.2*, <http://www.cims.nyu.edu/cmcl/fmm2dlib/fmm2dlib.html>, 2012.
- [12] T. KOCH AND J. LIESEN, *The conformal “bratwurst” maps and associated Faber polynomials*, Numer. Math., 86 (2000), pp. 173–191.
- [13] R. KRESS, *A Nyström method for boundary integral equations in domains with corners*, Numer. Math., 58 (1990), pp. 145–161.
- [14] ———, *Boundary integral equations in time-harmonic acoustic scattering*, Math. Comput. Modelling, 15 (1991), pp. 229–243.
- [15] H. KRÜGER AND B. SIMON, *Cantor polynomials and some related classes of OPRL*, J. Approx. Theory, 191 (2015), pp. 71–93.
- [16] N. S. LANDKOF, *Foundations of modern potential theory*, Springer-Verlag, New York-Heidelberg, 1972. Translated from the Russian by A. P. Doohovskoy, Die Grundlehren der mathematischen Wissenschaften, Band 180.
- [17] M. M. S. NASSER, *Numerical conformal mapping via a boundary integral equation with the generalized neumann kernel*, SIAM J. Sci. Comput., 31 (2009), pp. 1695–1715.
- [18] ———, *Fast solution of boundary integral equations with the generalized Neumann kernel*, Electron. Trans. Numer. Anal., 44 (2015), pp. 189–229.
- [19] M. M. S. NASSER AND F. A. A. AL-SHIHRI, *A fast boundary integral equation method for conformal mapping of multiply connected regions*, SIAM J. Sci. Comput., 35 (2013), pp. A1736–A1760.
- [20] M. M. S. NASSER AND C. C. GREEN, *Fast numerical methods for describing ideal fluid flow in domains with multiple stirrers*, in preparation, (2016).
- [21] M. M. S. NASSER, J. LIESEN, AND O. SÈTE, *Numerical computation of the conformal map onto lemniscatic domains*, Comput. Methods Funct. Theory, (2016), pp. 1–27.
- [22] M. M. S. NASSER, A. H. M. MURID, AND Z. ZAMZAMIR, *A boundary integral method for the Riemann–Hilbert problem in domains with corners*, Complex Var. Elliptic Equ., 53 (2008), pp. 989–1008.
- [23] T. RANSFORD, *Potential theory in the complex plane*, vol. 28 of London Mathematical Society Student Texts, Cambridge University Press, Cambridge, 1995.
- [24] ———, *Computation of logarithmic capacity*, Comput. Methods Funct. Theory, 10 (2010), pp. 555–578.
- [25] T. RANSFORD AND J. ROSTAND, *Computation of capacity*, Math. Comp., 76 (2007), pp. 1499–1520.
- [26] A. RATHSFELD, *Iterative solution of linear systems arising from the Nyström method for the double-layer*

- potential equation over curves with corners*, Math. Methods Appl. Sci., 16 (1993), pp. 443–455.
- [27] J. ROSTAND, *Computing logarithmic capacity with linear programming*, Experiment. Math., 6 (1997), pp. 221–238.
- [28] E. B. SAFF, *Logarithmic potential theory with applications to approximation theory*, Surv. Approx. Theory, 5 (2010), pp. 165–200.
- [29] K. SCHIEFERMAYR, *Estimates for the asymptotic convergence factor of two intervals*, J. Comput. Appl. Math., 236 (2011), pp. 28–38.
- [30] O. SÈTE AND J. LIESEN, *On conformal maps from multiply connected domains onto lemniscatic domains*, Electron. Trans. Numer. Anal., 45 (2016), pp. 1–15.
- [31] ———, *Properties and Examples of Faber–Walsh Polynomials*, Comput. Methods Funct. Theory, (2016), pp. 1–27.
- [32] G. SZEGÖ, *Bemerkungen zu einer Arbeit von Herrn M. Fekete: Über die Verteilung der Wurzeln bei gewissen algebraischen Gleichungen mit ganzzahligen Koeffizienten*, Math. Z., 21 (1924), pp. 203–208.
- [33] J. L. WALSH, *On the conformal mapping of multiply connected regions*, Trans. Amer. Math. Soc., 82 (1956), pp. 128–146.
- [34] E. T. WHITTAKER AND G. N. WATSON, *A course of modern analysis. An introduction to the general theory of infinite processes and of analytic functions: with an account of the principal transcendental functions*, Fourth edition. Reprinted, Cambridge University Press, New York, 1962.